Penerbit Akademia Baru

CFD Letters

Journal homepage: www.akademiabaru.com/cfdl.html
ISSN: 2180-1363

Study of Turbulence Model for Performance and Flow Field Prediction of Pico Hydro Types Propeller Turbine

Open Access

Warjito[1], Sanjaya BS Nasution[1], Muhammad Farhan Syahputra[1,*], Budiarso[1], Dendy Adanta[1]

[1] Department of Mechanical Engineering, Faculty of Engineering, Universitas Indonesia, Depok 16242, West Java, Indonesia

ARTICLE INFO

Article history:
Received 20 June 2020
Received in revised form 19 August 2020
Accepted 24 August 2020
Available online 30 August 2020

ABSTRACT

The computational fluid dynamics (CFD) method is a method often used in predicting the performance and flow field of turbine because it is cheap and fast. The accuracy of CFD method is influenced by several aspects: boundary conditions, discretization of space and time method, and the use of turbulence models. For turbulence model, there is no clarity of the most accurate model, especially in the pico hydro type propeller. Therefore, this study compared three turbulent models based on Reynolds Average Navier-Stokes (RANS) two equations to predicts the performance of a pico hydro propeller turbine: standard k-ε, Group Normalization (RNG) k-ε, and Shear Stress Transport (SST) k- ω. This study used a three-dimensional simulation method, transient, and six-degree of freedom features. The Grid Convergency index (GCI) and Time-step Independence Index (TCI) were used to verify the simulation results. From the results, the CFD results were similar to the experiment results (valid). Furthermore, there was different prediction of performance due to differences in the turbulence model but not too high. Based on this, for prediction of performance pico hydro propeller turbine, the standard k-ε turbulence model was recommended for use. However, for study flow field, RNG k-ε and SST k-ω were recommended because they were not over-predicted in the dissipation rate calculation.

Keywords:
Pico hyro; propeller turbine; computation; RANS; turbulence model

1. Introduction

In 2018, approximately more than 5 million people in Indonesia do not yet have access to electricity [1]. Most of the electrification problems are in remote areas. This is caused by difficult access, so the cost of electricity connection from remote areas to the main grid is expensive [2]. To solve this problem, the government of Indonesia distributes diesel engines to remote areas [3]. This solution is considered ineffective because fuel must be distributed continuously. A possible solution is off-grid system using independent power plant based on renewable energy such as pico hydro, wind turbine and solar photovoltaic. The pico hydro is highly considered because Indonesia has a hydro power potential up to 19 GW in pico scale [3-5].

* *Corresponding author.*
E-mail address: syahputramuhammadfarhan@gmail.com (Muhammad Farhan Syahputra)

https://doi.org/10.37934/cfdl.12.8.2634

Pico hydro turbine is hydropower that produces power less than 5 kW. The advantages of pico hydro are it is easy to manufacture and has low maintenance cost [6]. One type of pico hydro turbine that can be used in remote areas is propeller turbine. The propeller turbine is categorized as reaction turbines which have performance relatively high and stable in low head conditions because a wide range of specific speed (N_s) [7-9]. The propeller turbine is a turbine that has a high modularity and compact so that it is able to be easily distributed to remote areas [7].

Since of its great benefits, several studies were conducted to improve the performance propeller turbine. Singh *et al.,* [10] explained that the blade length has more influence on the performance of the propeller turbine than the number of blades. Byeon and Kim [11] explained that propeller turbine with 4 number of blades is more effective than 3 and 5 number of blades. Podnar *et al.,* [12] compared two different hydrofoils and proposed a method to determine cavitation in propeller turbine using computer aided visualization. In addition, Podnar *et al.,* [12] suggest to be more selective in determining blade profile, because it affects the formation of cavitation (reducing efficiency). Simpson and Williamson [13] developed the manufacture method of pico scale hydropower propeller turbine for remote areas. The study found that incorrect correspondence between turbine rotor design and flow rate at the site significantly influenced turbine operation [13]. Alexander [14] compared 4 different propeller turbine runners designed with 4 different specific speed. The study explained that propeller turbine with *Ns* 242 was the most efficient runner compared to Ns 176, 355, and 544. Nasution *et al.,* [15] suggested to design propeller turbine runner based on Ns with a power function than discharge function. Based on numerical analysis, the runner designed based power function had better performance [15]. Adanta *et al.,* [9] explained that the distance between blades could change the flow velocity at the outlet where this made torque decrease causing the reduction of efficiency.

From the results of the review, the computational fluid dynamics (CFD) method is a widely used method. It is because it is able to reduce time and cost compared to experiment method and it shows a more detailed and extensive fluid phenomenon when compared to analytical method [16-17]. Furthermore, there are several aspects related to CFD accuracy; boundary condition, discretization of space and time method, and turbulence models [16-18]. Errors caused by boundary conditions can be eliminated if adjusted to be similar to the actual conditions. Discretization errors can be reduced by independency tests [19-20]. However, for turbulence model errors, there is no clarity of the most accurate model to use, especially in the case of turbomachinery.

In term of turbulence model, Božić and Benišek [21] compared SST k-ω with the Reynolds stress model (RSM) to calculate profile and secondary losses. The results of the study revealed that the values of total and profile losses were lower and more accurate using the SST k-ω turbulence model [21]. Furthermore, Siswantara *et al.,* [22] have conducted the comparison of six turbulence models in crossflow turbine. All the turbulence models are standard wall function k-ε, scalable wall function k-ε, standard wall function RNG, scalable wall function RNG, standard transitional SST, and transitional SST with curvature corrections [22]. The results showed that there was a difference prediction of runner performances but not high [22]. Based on the results, the transitional SST turbulent models were optimum [22].

Based on Siswantara *et al.,* [22] study, turbulent models affect the predictions for turbomachinery cases. Consequently, to determine the suitable turbulence model in propeller turbine in pico scale, a study is needed. Therefore, the purpose of this study is to compare three Reynolds Average Navier-Stokes (RANS) turbulence models. Turbulence models based on RANS were chosen because they are the most widely used because of their fairly good accuracy and relatively moderate use of computer power [23]. The turbulence models compared were standard k-ε, Renormalization Group (RNG) k-ε, and Shear Stress Transport (SST) k-ω.

2. Methodology

2.1 Geometry

The blade and draft-tube geometry in this study were the same as the geometry used by Ho-Yan [7]. Ho-Yan's [7] study was used because it showed more complete methods and results so that it can be used as a validator. The following is Table 1 and Figure 1 which are the main parameters of blade and draft-tube geometry.

Table 1
Main design parameters

Parameters	Value
Number of blades, z	4
Outer diameter, D_o	130 mm
Inner diameter, D_i	70 mm
Tip chord length, L	109 mm
Hub chord length, L	74 mm
Blade's angle, β	25.54°
Inlet Diameter, D_{in}	141.3 mm
Outlet Diameter, D_{out}	298.06 mm
Draft tube height, T	1700 mm

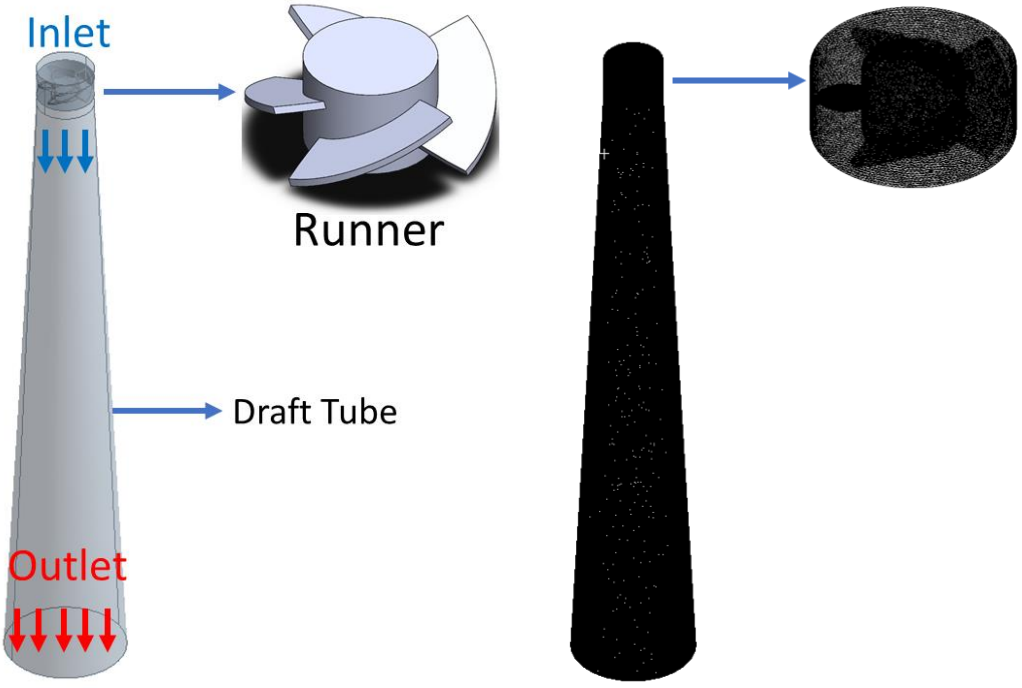

(a) (b)

Fig. 1. Simulation setup (a) schematic of boundary condition (b) visualization of mesh

2.2 Simulation Setup

The computation was run by applying the ANSYS™ FLUENT® 18.1 software. The six-degrees of freedom (6-DoF) feature was used to get the computational results close to the actual conditions because this feature could predict the runner rotation [24]. The 6-DoF is a solver for calculating external forces and moments such as gravitational force and moments on an object where this solver is a transient dynamic mesh simulation [25]. Therefore, the rotation of the propeller turbine is the

computation result (dependent variable) and it is different from standard moving mesh and multi reference frame (MRF) which rotation was defined in boundary condition. Furthermore, the mesh type used was tetrahedron because this type was suitable for complex geometry such as runner of propeller turbine (see Figure 1(b)).

There were several simulation setups used. Pressure based solver was chosen because the flow is incompressible. There was an influence of body force (g_y = -9,8 m/s^2). The Inlet condition is mass flow with 12.9 l/s. The outlet condition is pressure outlet with 0 Pa. The runner object was set to be a moving wall. The dynamic mesh activation settings were smoothing mesh method and 6-DoF option. The settings of 6-DoF were one DoF rotation with moment of inertia of 0.02 kg·m^2 and preload of -0.02 N. m. The moment of inertia value could be found from computer aided software. Solution method is SIMPLE because this needed computing power lower than others.

2.3 Reynolds Average Navier-Stokes (RANS)

Three turbulence models were based on RANS with two equations for compared: standard k-ε, RNG k-ε, and SST k-ω. These three models are most often used for industrial and educational purposes.

The governing equations of the standard k-ε turbulence model are Eq. (1) for kinetic energy turbulent and Eq. (2) for dissipation rate [25]:

$$\frac{\partial}{\partial t}(\rho k)+\frac{\partial}{\partial x_i}(\rho k u_i)=\frac{\partial}{\partial x_j}\left[\left(\mu+\frac{\mu_t}{\sigma_k}\right)\frac{\partial}{\partial x_j}\right]+G_k+G_b-\rho\varepsilon-Y_M+S_k \tag{1}$$

$$\frac{\partial}{\partial t}(\rho \varepsilon)+\frac{\partial}{\partial x_i}(\rho \varepsilon u_i)=\frac{\partial}{\partial x_j}\left[\left(\mu+\frac{\mu_t}{\sigma_\varepsilon}\right)\frac{\partial \varepsilon}{\partial x_j}\right]+C_{1\varepsilon}\frac{\varepsilon}{k}(G_K+C_{3\varepsilon}G_b)-C_{2\varepsilon\rho}\frac{\varepsilon^2}{k}+S_\varepsilon \tag{2}$$

where μ_t is turbulence viscosity; G_k and $G_b$are the generation of turbulence kinetic energy due to the mean velocity gradients and buoyancy, respectively; Y_M represents the contribution of the fluctuating dilatation in compressible of turbulence to the overall dissipation rate; σ_k and σ_ε are inverse-turbulent Prandtl numbers for k and ε, respectively;$C_{1\varepsilon}$, $C_{2\varepsilon}$ and $C_{3\varepsilon}$is constant; $S_k$and S_ε are user defined source terms.

The governing equations of the RNG k-ε turbulence models are Eq. (3) for kinetic energy turbulent and Eq. (4) for dissipation rate [25]:

$$\frac{\partial}{\partial t}(\rho k)+\frac{\partial}{\partial x_i}(\rho k u_i)=\frac{\partial}{\partial x_j}\left(\alpha_k \mu_{eff}\frac{\partial k}{\partial x_j}\right)+G_k+G_b-\rho\varepsilon-Y_M+S_k \tag{3}$$

$$\frac{\partial}{\partial t}(\rho \varepsilon)+\frac{\partial}{\partial x_i}(\rho \varepsilon u_i)=\frac{\partial}{\partial x_j}\left(\alpha_k \mu_{eff}\frac{\partial \varepsilon}{\partial x_j}\right)+C_{1\varepsilon}\frac{\varepsilon}{k}(G_K+C_{3\varepsilon}G_b)-C_{2\varepsilon\rho}\frac{\varepsilon^2}{K}+S_\varepsilon \tag{4}$$

The governing equations of the of the SST k-ω turbulence model are Eq. (5) for kinetic energy turbulent and Eq. (6) for specific dissipation rate (ω) [25]:

$$\frac{\partial}{\partial t}(\rho k)+\frac{\partial}{\partial x_i}(\rho k u_i)=\frac{\partial}{\partial x_j}\left(\Gamma_k\frac{\partial k}{\partial x_j}\right)+G_k-Y_k+S_k \tag{5}$$

$$\frac{\partial}{\partial t}(\rho \omega)+\frac{\partial}{\partial x_i}(\rho \omega u_i)=\frac{\partial}{\partial x_j}\left(\Gamma_\omega\frac{\partial \omega}{\partial x_j}\right)+G_\omega-Y_\omega+D_\omega+S_\omega \tag{6}$$

where Γ_k and Γ_ω are effective diffusivity ok *k* and ω, respectively.

2.4 Independency Test

The optimum mesh number was determined by using grid convergence index (GCI) calculation method. The GCI calculation is based on the Richardson extrapolation method [24-25]. The torque (τ) was variable that was used as an independency test data which was compared in each variation of the number of mesh. The GCI analysis was performed on the fine mesh to medium and medium to coarse. Eq. (7) was used to calculate GCI [26-27].

$$GCI_{12} = s_f \; x \left| \frac{1}{\tau_f} \frac{\tau_m - \tau_f}{r_{12}{}^{T_n} - 1} \right| x \; 100\% \tag{7}$$

where s_f is safety factor of 1.25, r is ratio of grid refinement, and T_n is order of convergence observed. *r* was determined by using the following [26-27]:

$$r_{12} = \left(\frac{M_f}{M_m} \right)^{0.5} \tag{8}$$

where M is mesh number. T_n was determined by the following way [26-27]:

$$T_{n+1} = ln \left[\left(\frac{\tau_c - \tau_m}{\tau_m - \tau_f} (r_{12}{}^{T_n} - 1) \right) + r_{12}{}^{T_n} \right] / \ln(r_{12} \cdot r_{23}) \tag{9}$$

Furthermore, since there is not yet standard method in determining the optimum discrete time, the GCI analysis was adopted to determine the optimum discrete time called the timestep convergence index (TCI).

3. Results and Discussions

3.1 Results

The variation of element numbers used were 318306, 691996, and 1460865 elements. The grid element ratios (r) were 2.17 and 2.11. The GCI calculation results are shown in Table 2. Based on Table 2, the mesh with 1460865 elements was used because it has an error below 1%. For the time step independency, the variation of discrete time were 0.001 s, 0.002 s, and 0.005 s, which corresponded to the frequency of 1000 Hz, 2500 Hz, and, 5000 Hz, respectively. The TCI calculation results are shown in Table 3. Based on Table 3, the time step frequency of 2500 Hz was used.

Table 2
GCI results

Normalized Grid Spacing	Number of Mesh	Torque, τ (N·m)	r	T	GCI (%)
2.14	318306	0.806	-	-	-
1.45	691996	0.835	1.47	-	0.718
1	1460865	0.839	1.45	5.0305	0.109
0	Δx→0	0.839	-	-	-

Table 3
TCI results

Normalized Timestep Spacing	Frequency (Hz)	Torque, τ (N·m)	r	T	GCI (%)
2.24	1000	0.315	-	-	-
1.41	2500	0.314	1.58	-	1.03
1	5000	0.313	1.41	0.86	0.76
0	Δt→Continuum	0.311	-	-	-

3.2 Turbulence Model Assessments

Figure 2 describes the computational results compared with experiment result based on Ho-Yan's study [7]. Figure 2(a) is a comparison graph between P (power) vs U/ C_1. U is runner velocity and C_1 is absolute velocity of water. From the Figure 2(a), the CFD results was valid because they were similar to Ho-Yan's [7] study. Figure 2(a) shows that the maximum power generated by the blade was at U/ C_1 between 0.2-0.3. Then, Figure 2(b) is a comparison graph between η (efficiency) vs U/ C_1. Figure 2(b) shows that the increasing of U/ C_1 reduced the torque.

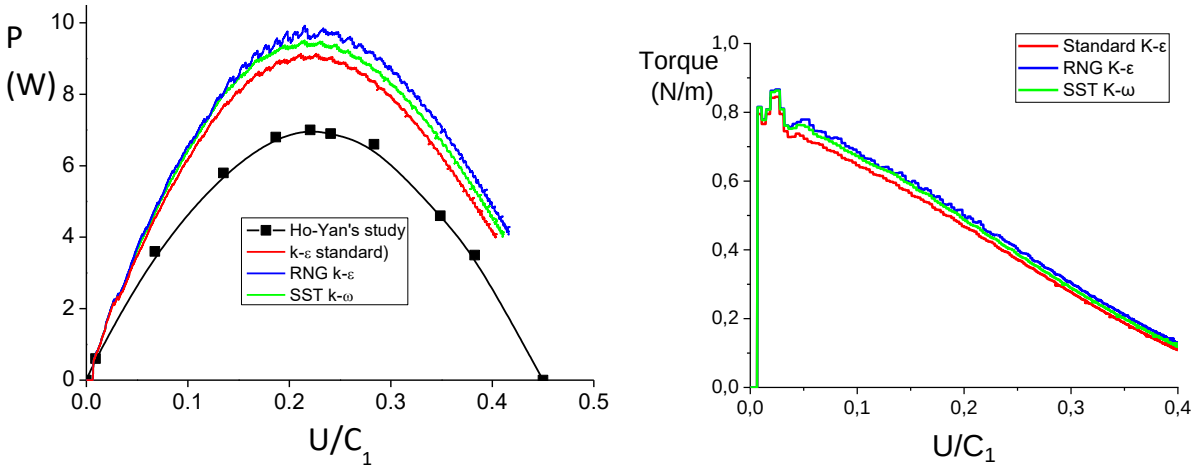

(a) (b)

Fig. 2. Simulation results (a) P vs U/C_1 (b) η vs U/C_1

3.3 Discussions

Based on Figure 2, there was difference result though it was not high. All varied turbulence models can be said relatively similar to predicted power and torque values for each variation of U / C_1. These results were similar to the Siswantara's [22] study in the case of cross-flow hydro turbines. Siswantara's [22] study shows that the changes in the turbulent model (k-ε, SST, and RNG) was different but not high [22].

Figure 3 shows the pressure contour on the pressure surface of the blade. The mechanical power of the blade was generated by the different total pressure distribution on the pressure and suction side of the blade. From Figure 3, the pressure distribution on the pressure side of each blade was not so different (relatively similar) which caused the prediction of performance of blades in Figure 2 was not much different.

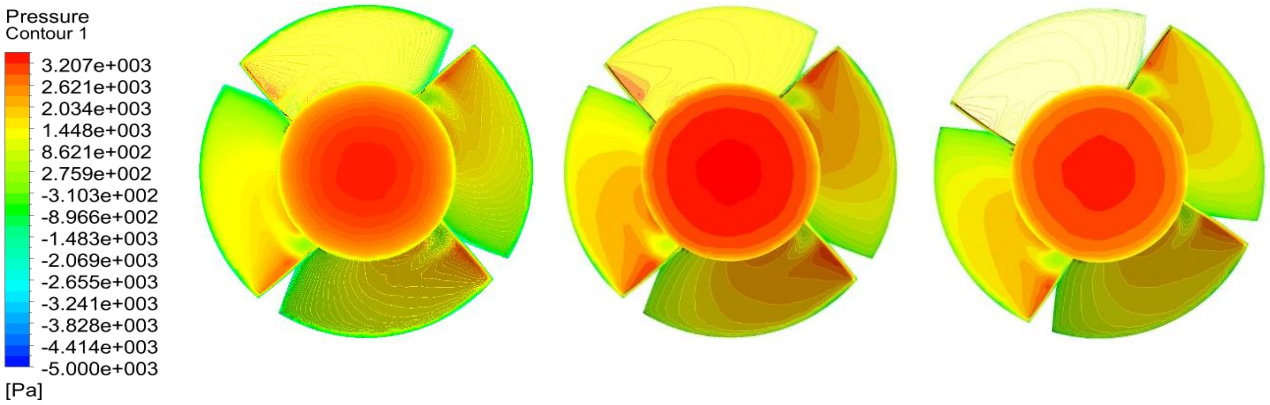

Fig. 3. Pressure contour on blade surface (a) legend (b) standard k-ε (c) RNG k-ε (d) SST k-ω

On the other hand, based on Figure 4, there were differences of flow phenomena in the draft tube. Based on Figure 4, prediction of flow in the standard k-ε model was longer than prediction of SST k-ω and RNG k-ε. The difference in the prediction of the three turbulent models was caused by the different assumption of the range of mixing length used by the three models.

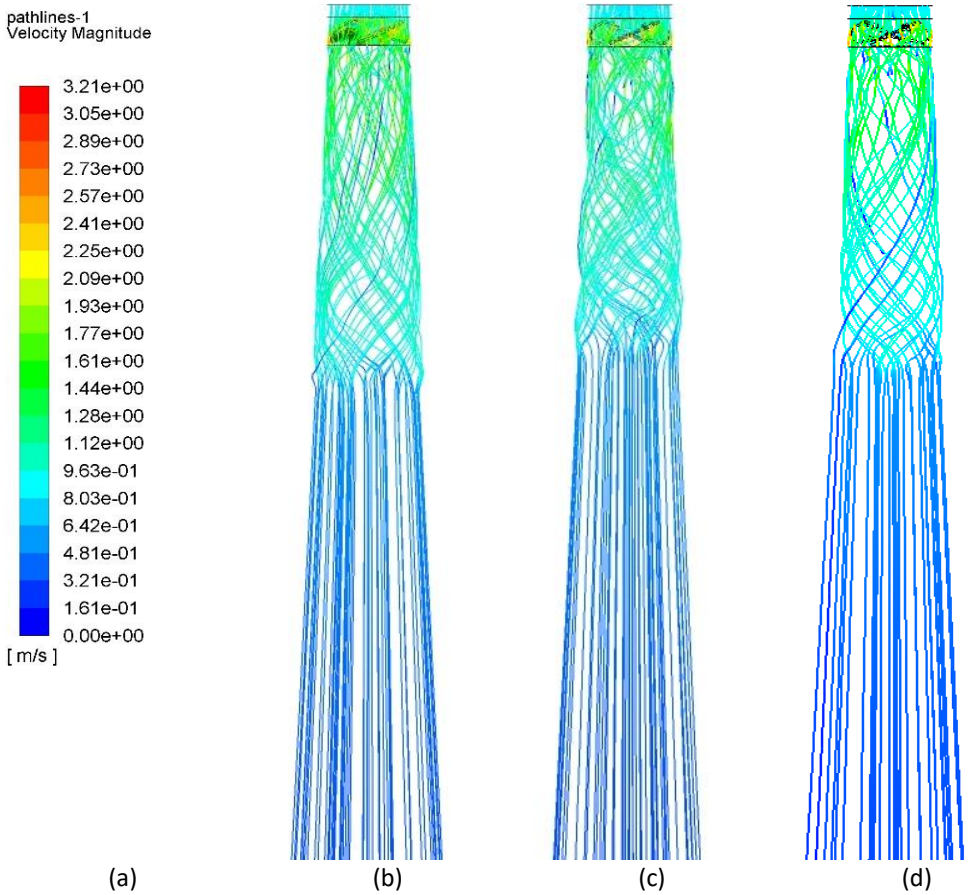

Fig. 4. Path line of velocity of water a) legend (b) standard k-ε (c) RNG k-ε (d) SST k-ω

Versteeg and Malalasekera [16] stated that the standard k-ε turbulence model predicted the high mixing length values than SST k-ω and RNG k-ε. This is why the standard k-ε turbulence model was over predicted when the flow was in the production regime and was too diffusive which can be seen in Figure 4(a). Figure 4(a) shows that the magnitude velocity of swirling flow was not higher compared

to the others (see Figure 4(b) and 4(c)). The length of prediction swirling ensures that the standard k-ε turbulence model was over predicted in calculating the dissipation rate.

The different predictions of the standard k-ε with RNG k-ε turbulent model was due to the equation of ε of RNG k-ε that had been modified for calculating the rotating flow effect (swirling) [28]. The RNG k-ε turbulence model was developed to correct over-predictions made by the standard k-ε [29-30]. As a result, the RNG k-ε was not too diffusive compared to the standard k-ε.

From Figures 2 and 3, the prediction of swirling flow between the SST k-ω and the RNG k-ε turbulence model was similar (insignificantly different). The SST k-ω turbulence model was developed to improve the prediction of swirling flow. This improvement occurs due to the modelling of shear stress between boundary layer which was proportional to the turbulence kinetic energy [31-32]. This is the reason for the chaotic and fluctuating behaviour of the flow. The SST k-ω turbulence model was a good preference because the measurement of the adverse flow was more precise than the standard k-ω turbulence model.

4. Conclusions

Predictions of comparative performance of propeller turbine in pico scale using three turbulence models based on RANS two equations (standard k-ε, RNG k-ε, and SST k-ω) had been carried out. From the results, there was different prediction of performance due the variation of turbulence model but not too high. For prediction of performance propeller turbine in pico scale, the standard k-ε turbulence model was recommended to use. However, for study flow field, RNG k-ε and SST k-ω were recommended because they were not over-predicted in calculating the dissipation rate.

Acknowledgement

This work was supported by the Ministry of Research, Technology, and Higher Education (KEMENRISTEK DIKTI) of Republic of Indonesia with grant No: NKB-1631/UN2.R3.1/HKP.05.00/2019.

References

[1] Kementerian ESDM. "Rasio Elektrifikasi Indonesia Tahun 2018." (2018).
[2] Kaunda, Chiyembekezo S., Cuthbert Z. Kimambo, and Torbjorn K. Nielsen. "A technical discussion on microhydropower technology and its turbines." *Renewable and Sustainable Energy Reviews* 35 (2014): 445-459. https://doi.org/10.1016/j.rser.2014.04.035
[3] Munasinghe, Mohan. "Rural electrification in the Third World." *Power Engineering Journal* 4, no. 4 (1990): 189-202. https://doi.org/10.1049/pe:19900038
[4] Williams, Arthur, and Stephen Porter. "Comparison of hydropower options for developing countries with regard to the environmental, social and economic aspects." *in International Conference on Renewable Energy for Developing Countries*, 2006.
[5] Kementerian PU. "Potensi PLTA Di Indonesia." (2014).
[6] Energy Sector Management Assistance Program. "Technical and economic assessment of off grid, mini-grid and grid electrification technologies." (2007).
[7] Ho-Yan, Bryan. "Design of a low head pico hydro turbine for rural electrification in Cameroon." PhD diss., University of Guelph, 2012.
[8] Nechleba, Miroslav. *Hydraulic turbines, their design and equipement*. No. BOOK. Artia, 1957.
[9] Adanta, D., Emanuele Quaranta, and T. M. I. Mahlia. "Investigation of the effect of gaps between the blades of open flume Pico hydro turbine runners." *Journal of Mechanical Engineering and Sciences* 13, no. 3 (2019): 5493-5512. https://doi.org/10.15282/jmes.13.3.2019.18.0444
[10] Singh, Punit, and Franz Nestmann. "Experimental investigation of the influence of blade height and blade number on the performance of low head axial flow turbines." *Renewable Energy* 36, no. 1 (2011): 272-281. https://doi.org/10.1016/j.renene.2010.06.033
[11] Byeon, Sun-Seok, and Youn-Jea Kim. "Influence of blade number on the flow characteristics in the vertical axis propeller hydro turbine." *International Journal of Fluid Machinery and Systems* 6, no. 3 (2013): 144-151.

https://doi.org/10.5293/IJFMS.2013.6.3.144
[12] Podnar, Andrej, Matevž Dular, Brane Širok, and Marko Hočevar. "Experimental analysis of cavitation phenomena on Kaplan turbine blades using flow visualization." *Journal of Fluids Engineering* 141, no. 7 (2019). https://doi.org/10.1115/1.4041985
[13] Simpson, R. G., and A. A. Williams. "Application of computational fluid dynamics to the design of pico propeller turbines." In *Proceedings of the international conference on renewable energy for developing countries*, pp. 5-7. University of the District of Columbia Washington, DC, 2006.
[14] Alexander, K. V., E. P. Giddens, and A. M. Fuller. "Axial-flow turbines for low head microhydro systems." *Renewable energy* 34, no. 1 (2009): 35-47. https://doi.org/10.1016/j.renene.2008.03.017
[15] Nasution, S. B., Warjito Budiarso, and Dendy Adanta. "A Comparison of Openflume Turbine Designs with Specific Speeds (Ns) Based on Power and Discharge Functions." *Journal of Advanced Research in Fluid Mechanics and Thermal Sciences* 51, no. 1 (2018): 53-60.
[16] Versteeg, Henk Kaarle, and Weeratunge Malalasekera. *An introduction to computational fluid dynamics: the finite volume method*. Pearson education, 2007.
[17] De Andrade, Jesús, Christian Curiel, Frank Kenyery, Orlando Aguillón, Auristela Vásquez, and Miguel Asuaje. "Numerical investigation of the internal flow in a Banki turbine." *International Journal of Rotating Machinery* 2011 (2011). https://doi.org/10.1155/2011/841214
[18] Mockmore, Charles Arthur, and Fred Merryfield. "The Banki water turbine." (1949).
[19] Richards, Shane A. "Completed Richardson extrapolation in space and time." *Communications in numerical methods in engineering* 13, no. 7 (1997): 573-582. https://doi.org/10.1002/(SICI)1099-0887(199707)13:7<573::AID-CNM84>3.0.CO;2-6
[20] Nasution, Sanjaya, and Dendy Adanta. "Effect of tangential absolute velocity at outlet on open flume turbine performance." *in IOP Conference Series: Earth and Environmental Science*, vol. 431, no. 1, p. 12023, 2020. https://doi.org/10.1088/1755-1315/431/1/012023
[21] Božić, Ivan, and Miroslav Benišek. "An improved formula for determination of secondary energy losses in the runner of Kaplan turbine." *Renewable Energy* 94 (2016): 537-546. https://doi.org/10.1016/j.renene.2016.03.093
[22] Siswantara, Ahmad Indra, Aji Putro Prakoso Budiarso, Gun Gun R. Gunadi, and Dendy Warjito. "Assessment of turbulence model for cross-flow pico hydro turbine numerical simulation." *CFD Lettets* 10, no. 2 (2018): 38-48.
[23] Adanta, Dendy, Warjito Budiarso, and Ahmad Indra Siswantara. "Assessment of turbulence modelling for numerical simulations into pico hydro turbine." *Journal of Advanced Research in Fluid Mechanics and Thermal Sciences* 46, no. 1 (2018): 21-31.
[24] Prakoso, Aji Putro, Ahmad Indra Siswantara, and Dendy Adanta. "Comparison between 6-DOF UDF and moving mesh approaches in CFD methods for predicting cross-flow pico-hydro turbine performance." *CFD Letters* 11, no. 6 (2019): 86-96.
[25] A. F. U. Guide. "Release 17.0."*Ansys Inc*, 2016.
[26] Roache, Patrick J. *Verification and validation in computational science and engineering*. Vol. 895. Albuquerque, NM: Hermosa, 1998.
[27] Roache, Patrick J. "Quantification of uncertainty in computational fluid dynamics." *Annual review of fluid Mechanics* 29, no. 1 (1997): 123-160. https://doi.org/10.1146/annurev.fluid.29.1.123
[28] L. Davidson. *Fluid mechanics, turbulent flow and turbulence modeling*. Chalmes University of Technology, 2015.
[29] Yakhot, Victor, and Steven A. Orszag. "Renormalization group analysis of turbulence. I. Basic theory." *Journal of scientific computing* 1, no. 1 (1986): 3-51. https://doi.org/10.1007/BF01061452
[30] S. A. Orszag and V. Yakhot. "Renormalization Group Analysis of Turbulence." in *Proceedings of the International Congress of Mathematicians*, pp. 1395–1399, 1986.
[31] Menter, F. R. *Improved two-equation k–omega turbulence models for aerodynamic flows-NASA Technical Memorandum TM-103975*. Technical report, NASA, Ames, CA, 1992.
[32] Menter, Florian R. "Zonal two equation kw turbulence models for aerodynamic flows." In *23rd fluid dynamics, plasmadynamics, and lasers conference*, p. 2906. 1993. https://doi.org/10.2514/6.1993-2906